International Journal of Control and Automation
Vol. 9, No. 12 (2016), pp. 427-438
http//dx.doi.org/10.14257/ijca.2016.9.12.35

Wideband Stochastic Chaotic Signal and Its Application for Radar Imaging

Jun Tang[1,2]

[1]*Department of Communication Engineering, Xiamen University of Technology, Xiamen 361024, China*
[2]*Department of Communication Engineering, School of Information Science and Engineering, Xiamen University, Xiamen 361024, China*
xmtangjun@126.com

Abstract

A novel model of stochastic chaotic radar waveform with stochastically stepped carrier frequencies is proposed, in which, a nonlinear system generating an unpredictable aperiodic stochastic chaotic signal (SCS) is used to control stepping of carrier frequencies. The stochastic chaotic frequency-modulation (SCFM) signal is used as the baseband noise signal, which is truly random and has a thumbtack ambiguity function (AF). SCS can be used to estimate velocity and for imaging of high-speed targets. Wideband signal is obtained by coherently synthesizing for high-resolution range (HRR) imaging. Finally, numerical simulations show the effectiveness of the proposed signal model and corresponding algorithms.

Keywords*: stochastic chaotic, noise radar, velocity estimation, stepped frequency*

1. Introduction

Random signal radar (RSR) has "thumbtack" ambiguity function with high-resolution of in range and speed as well as high measurement accuracy [1, 2]. The advantages of RSR are strong anti-interference ability, low probability of intercept, good electromagnetic compatibility, etc [3, 4]. Although random noise has an excellent autocorrelation function, its generation, replication and control process are very complicated. Consequently, it is difficult to obtain an ideal noise signal. Instead, a pseudo-random signal is utilized as noise radar signal source.

Chaotic signals show noise-like characteristics, and many excellent radar waveforms have been designed using existing chaotic systems. In addition, wideband radar signals are obtained by chaotic modulation. However, intrinsic deterministic nature of such systems determine the internal structure and determinacy of corresponding signals, and, strictly speaking, no true random waveform is available by this approach. Especially after different modulation, the properties of many modulated chaotic signals become poor and cannot be used for high resolution radar imaging. To improve the performance of radar waveforms, several improvements were made on existing systems by different means [5-11]. These include a chaos sampled method to reduce correlation between samples [5], a waveform design based on Lorenz system by adjusting parameter [7, 8], and obtaining expected chaotic sequences by modifying existing chaotic systems [9, 10]. All these methods lack strict systematic theory and universality.

To achieve high-resolution radar imaging, a wideband signal is required. [12] proposed stepped-frequency signal, which can synthesize bandwidth, but its ambiguity function has high sidelobes [13]. To overcome this shortcoming, [14] proposed stepped-frequency Chirp signal (SFCS), but SFCS is sensitive to coherent jamming [15]. Later, noise signal took the place of chirp signal, then the stepped-frequency noise signal (SFNS) came out

ISSN: 2005-4297 IJCA

[16-19].

In order to get accurate velocity estimation, we adopt a new search method based on the AF of SCFM signal, which consists of a two-stage process: a rough search followed by an accurate search. The former can ensure the estimation error no more than the velocity resolution, and the latter can get an accurate velocity estimation by using the golden section search (GSS) algorithm.

2. Stochastic Chaotic Signal

Stein and Ulam were the first to prove [20]

$$X_n = \sin^2\left(\theta\pi 2^n\right) \tag{1}$$

is a general solution to the Logistic map, n is a natural number and θ is a non-zero real number. Since then, more and more exact solutions to other chaotic maps have been found [20], and all those can be written in a general form

$$X_n = P\left(\theta T z^n\right) \tag{2}$$

where $P(\square)$ is a periodic function with the period T, z is an integral number, and $P(\theta T)$ defines the initial value. Since Eq. (2) is a deterministic process, when z is an integral number, X_n in Eq. (2) will be a deterministic sequence as well. When z is non-integer, however, X_n will be quite different [22].

Assume that $z = p/q$ is a rational number, p and q are co-prime. It can be proved that if there are $m+1$ samples (m is an arbitrary natural number) $X_0, X_1, X_2, \ldots, X_m$ generated from Eq.(2), one cannot predict the value of the next sample.

We define the sequences parameterized by integral number k as follows:

$$X_n^{(k,m)} = \sin^2\left[\pi\left(\theta_0 + q^m k\right)\left(\frac{p}{q}\right)^n\right] \tag{3}$$

The first $m+1$ values are the same since that

$$X_n^{(k,m)} = \sin^2\left[\pi\theta_0\left(\frac{p}{q}\right)^n + \pi k p^n q^{m-n}\right] = \sin^2\left[\pi\theta_0\left(\frac{p}{q}\right)^n\right] \tag{4}$$

holds for all $n \le m$. So there are infinite sequences which have same first $m+1$ values. However, the value of the next point

$$X_{m+1}^{(k,m)} = \sin^2\left[\pi\theta_0\left(\frac{p}{q}\right)^{m+1} + \pi k\frac{p^{m+1}}{q}\right] \tag{5}$$

is uncertain. Generally, $X_n^{(k,m)}$ can take q different values, which means that $X_n^{(k,m)}$ is forward unpredictable. It can be proved that $X_n^{(k,m)}$ is backward unpredictable as well.

The sequence family is defined as

$$X_n^{(k,m,s)} = \sin^2\left[\pi\left(\theta_0 + q^m k\right)\left(\frac{q}{p}\right)^s\left(\frac{p}{q}\right)^n\right] \tag{6}$$

where k, m, s are integral numbers. The value X_{s-1} is uncertain with the known string $X_s, X_{s+1}, X_{s+2}, \ldots, X_{s+m}$, since

$$X_{s-1}^{(k,m,s)} = \sin^2\left[\pi\left(\theta_0 + q^m k\right)\left(\frac{q}{p}\right)^s\left(\frac{p}{q}\right)^{s-1}\right] = \sin^2\left(\pi\theta_0\frac{q}{p} + \pi k\frac{q^{m+1}}{p}\right) \tag{7}$$

Thus, X_{s-1} has p different possible values. When z is an irrational number, the past and future points can take infinite values. Therefore, such sequences have true randomness.

Based on the analysis of stochastic behavior in Eq. (2), which can be expressed in a

general form

$$X_n = P(\theta_0 h(n)) \tag{8}$$

where $h(n)$ is an exponential function and $P(\cdot)$ is a periodic function, which correspond to "stretching" and "folding" in generating mechanism of chaos respectively, and θ_0 is an initial value.

By popularizing the aforementioned idea to a continuous time system, we can construct an even simpler chaotic signal given by

$$X(t) = P\left(A\exp\left[Q(t)\right]\right) \tag{9}$$

where $P(\cdot)$ is a periodic function and $Q(\cdot)$ is bounded a pseudo-periodic function. Consequently, $A\exp\left[Q(t)\right]$ oscillates aperiodically within an interval.

According to Eq. (9), we can construct a stochastic chaotic signal, whose Lyapunov exponent can be calculated analytically as follows:

$$X(t) = \Phi(t)(\bmod 1) - 0.5 \tag{10}$$

$$Q(t) = E_1(t) + E_2(t) + E_3(t), E_i(t) = ct - ckT_i, kT_i \le t \le (k+1)T_i \tag{11}$$

where $\Phi(t) = \exp[Q(t)]$, $c, T_i > 0, i = 1,2,3$, k is an integral number, $T_2/T_1, T_3/T_2, T_3/T_1$ etc. are irrational numbers. The theoretical Lyapunov exponent of $X(t)$ is $\lambda = \ln 3c$ [23].

A time-series is generated by Eq. (10) with $c = 1, T_1 = \pi, T_2 = \sqrt{3} + 2, T_3 = 3$.

Figure 1 shows the waveform of $X(t)$ with initial value $\Phi(0) = 1.2$ and 1.20001 respectively. It can be seen from

Figure 1 that the trajectories of $X(t)$ are sensitive to the initial values.

Figure 2 is the first-return map of $X(t)$. For notational convenience, $X(t)$ is noted as SCS (Stochastic Chaotic Signal) hereinafter.

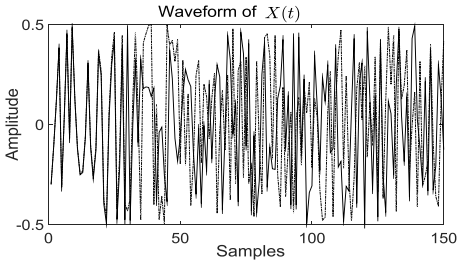

Figure 1. Stochastic Chaotic Signal Waveforms

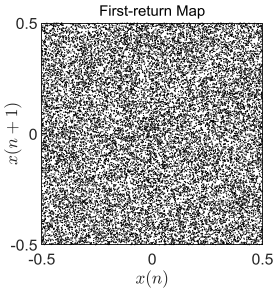

Figure 2. First-Return Map of Stochastic Chaotic Signal

3. Stochastic Chaotic Signals with Randomly Stepped Carrier Frequencies

Figure 3 depicts the generation procedure of wideband stochastic chaotic signal (WBSCS), in which frequency-hopping codes (FHC) and SCFM are generated from SCS, the former are used to control stepped carrier frequencies and latter to form WBSCS by frequency modulation.

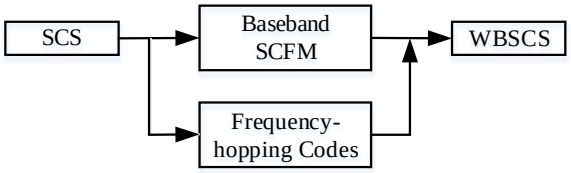

Figure 3. Generation Procedure of WBSCS

3.1. Baseband SCFM Signal

Firstly, the baseband noise SCFM signal by frequency modulation based on the SCS can be expressed as

$$g(t) = A\exp\left\{ j2\pi \int_0^t X(\tau)\, d\tau \right\} \tag{12}$$

The ambiguity function is always used to investigate radar signals for their resolution performance [24]. According to [25], we define the AF of $g(t)$ as follows

$$\left|\chi(\tau, f_d)\right|^2 = \left|\int_{-\infty}^{\infty} g^*(t)\, g(t-\tau) \exp(-j2\pi f_d t)\, dt\right|^2 \tag{13}$$

where τ, f_d are time delay and Doppler shift respectively.

Letting $f_d = 0$, we get the range cut of the AF

$$\left|\chi(\tau, 0)\right|^2 = \left|\int_{-\infty}^{\infty} g^*(t)\, g(t-\tau)\, dt\right|^2 \tag{14}$$

Letting $\tau = 0$, we obtain the Doppler frequency cut of the AF

$$\begin{aligned} \left|\chi(0, f_d)\right|^2 &= \left|\int_{-\infty}^{\infty} g^*(t)\, g(t) \exp(-j2\pi f_d t)\, dt\right|^2 = \left|\int_{-\infty}^{\infty} \left|g(t)\right|^2 \exp(-j2\pi f_d t)\, dt\right|^2 \\ &= \left|\int_{-T_p/2}^{T_p/2} A^2 \exp(-j2\pi f_d t)\, dt\right|^2 = \left| A^2 \frac{\sin(\pi f_d T_p)}{\pi f_d T_p} \right|^2 \end{aligned} \tag{15}$$

where T_p is the time duration (TD) of the SCFM signal. The Doppler resolution df_d is determined by T_p

$$df_d = \frac{1}{T_p} \tag{16}$$

The relation between v and f_d is

$$f_d = \frac{2vf_c}{c} \tag{17}$$

and the velocity resolution is

$$dv = df_d \cdot \frac{c}{2f_c} = \frac{c}{2f_c \cdot T_p} \tag{18}$$

3.2. Frequency-Hopping Code

For the range of SCS is $X_n \in [-1/2, 1/2]$, which cannot be used directly to control the steps of carrier frequencies. To map the SCS sequence to the range of FHC $c_n \in \{0,1,\cdots,N-1\}$, we define

$$X_n^* = \left\lfloor \left(X_n + \frac{1}{2} \right) * N \right\rfloor \tag{19}$$

where $\lfloor \cdot \rfloor$ round down to the nearest integer. In order to eliminate the correlation of X_n^*, we remove $m-1$ from every m values to get the following sequence

$$\hat{X}_n = X_{n*m}^*, \; n \in \left[0, \left\lfloor \frac{N}{m} \right\rfloor \right] \tag{20}$$

Then we just select the different values to form c_n.

3.3. Transmitted Signal

Stochastic chaotic signals with randomly stepped carrier frequencies include a set of subpulses with randomly stepped frequencies, and each subpulse is a narrowband stochastic chaotic signal.

Suppose f_0, Δf denote the start carrier frequency and frequency step, respectively. Then, carrier frequency of the N th subpulse is $f_n = f_0 + c_n \Delta f$, where $c_n \in \{0,1,\cdots,N-1\}$ is FHC and N is the number of subpulses.

The proposed signal model can be mathematically expressed as

$$\begin{aligned} & s(t) = g_n(\hat{t}) \cdot \exp(j2\pi f_n t) \cdot \mathrm{rect}\left(\frac{t - nT_r}{T_p} \right) \\ & \hat{t} = t - t_n, \quad 0 \le \hat{t} \le T_p \\ & t_n = nT_r, \quad n = 0,1,\cdots,N-1; \end{aligned} \tag{21}$$

where $g_n(\hat{t})$ is the n th subpulse, $\hat{t}$ fast-time, t_n the starting time of the n th subpulse, T_r the subpulse interval, T_p the duration of each subpulse, and rect(□) the rectangle window function

$$\mathrm{rect}(x) = \begin{cases} 1, & 0 \le x \le 1 \\ 0, & \text{otherwise} \end{cases} \tag{22}$$

3.4. Received Signal

Suppose all targets have a constant velocity v, and locate R_k $(k = 1,2,\cdots,K)$ m apart away from the radar. The instantaneous ranges are

$$R_k(t_n, \hat{t}) = R_k - v(t_n + \hat{t}) \tag{23}$$

Therefore, the received signal is

$$s_r(t_n, \hat{t}) = \sum_{k=1}^{K} A_k g_n \left[\hat{t} - \frac{2R_k(t_n, \hat{t})}{c} \right] \cdot \exp\left[j2\pi f_n \left(t - \frac{2R_k(t_n, \hat{t})}{c} \right) \right] \tag{24}$$

The baseband form of received signal is

$$\begin{aligned} s_{br}\left(t_n,\hat{t}\right) &= \sum_{k=1}^{K} A_k g_n\left[\left(1+\frac{2v}{c}\right)\hat{t}-\frac{2R_k}{c}+\frac{2vt_n}{c}\right] \\ &\quad \cdot\exp\left[-j2\pi f_n\left(\frac{2R_k}{c}-\frac{2v\left(t_n+\hat{t}\right)}{c}\right)\right] \\ &\approx \sum_{k=1}^{K}\tilde{A}_k g_n\left[\hat{t}-\frac{2R_k}{c}+\frac{2vt_n}{c}\right]\cdot\exp\left(\frac{j4\pi f_n vt_n}{c}\right)\cdot\exp\left(\frac{j4\pi f_n v\hat{t}}{c}\right) \end{aligned} \tag{25}$$

where $\tilde{A}_k = A_k\exp\left(-j4\pi f_n R_k/c\right)$. Frequency domain representation of baseband received signal is

$$S_{br}\left(t_n,f\right)=\left\{\sum_{k=1}^{K}\tilde{A}_k G_n\left(f-f_{dn}\right)\cdot\exp\left(\frac{-j4\pi fR_k}{c}\right)\cdot\exp\left[\frac{j4\pi\left(f+f_n\right)vt_n}{c}\right]\right\} \tag{26}$$

where $G_n(f)$ is the spectrum of $g_n(\hat{t})$, f_{dn} is the Doppler shift to f_n, $\exp\left(-j4\pi fR_k/c\right)$ is induced phase of the k th target owing to the initial range, $\exp\left(j4\pi f_n vt_n/c\right)$ is induced phase of the n th subpulse owing to the Doppler effect.

4. Velocity Estimation and Bandwidth Synthesis

4.1. Subpulse Compression and Velocity Estimation

Suppose v_{ref} and R_{ref} are the reference velocity and the reference range, respectively. In frequency domain, the reference signal can be expressed as

$$S_{ref}\left(t_n,f\right)=G_n\left(f-f_{dn\_ref}\right)\cdot\exp\left(\frac{-j4\pi fR_{ref}}{c}\right)\cdot\exp\left[\frac{j4\pi\left(f+f_n\right)v_{ref}t_n}{c}\right] \tag{27}$$

where f_{dn_ref} is the Doppler shift. Then, the output of matched filter is

$$\begin{aligned} S\left(t_n,f\right) &= S_{br}\left(t_n,f\right)\cdot S_{ref}^{*}\left(t_n,f\right) \\ &= \sum_{k=1}^{K}\tilde{A}_k G_n\left(f-f_{dn}\right)\cdot G_n^{*}\left(f-f_{dn\_ref}\right) \\ &\quad \cdot\exp\left[\frac{-j4\pi f\Delta R_k}{c}\right]\cdot\exp\left[\frac{j4\pi\left(f+f_n\right)\Delta vt_n}{c}\right] \end{aligned} \tag{28}$$

where $\Delta R_k = R_k - R_{ref}, \Delta v = v - v_{ref}$. The IFFT of $S\left(t_n,f\right)$ is

$$R_n = F^{-1}\left\{S\left(t_n,f\right)\right\} \tag{29}$$

4.1.1. Coarse Estimation of Velocity

In order to get credible results, we take N subpulses for consideration and average the matched-filtering results to get $\bar{R}_{peak}$. Suppose $\mathrm{RPM}=\bar{R}_{peak}/\bar{R}_{mean}$ denote the objective function, where $\bar{R}_{mean}$ is the average amplitude, and when

$$20*\lg\left(\mathrm{RPM}\right) > \mathrm{PSLR} \tag{30}$$

it is considered that $\left|v_{ref}-v\right| < dv$, where v_{ref} is reference velocity, v is the target velocity, dv is the velocity resolution, PSLR is the peak-sidelobe ratio of the CSFM signal.

4.1.2 Precise Estimation of Velocity

Since the mainlobe of SINC function has only one peak, we can get an accurate estimation of the velocity by the simple GSS algorithm [25]. The steps of GSS algorithm

are as follows:

1): Determine the initial velocities. If the target move toward the radar, the initial velocities is set as $v_a = v_c, v_b = v_c + dv$. Otherwise, the initial value is set as $v_a = v_c - dv, v_b = v_c$;

2): Let $x_1 = v_b - 0.618*(v_b - v_a)$ and $x_2 = x_a + 0.618*(v_b - v_a)$ as two reference velocities, respectively, then calculate $\bar{R}_{peak}(x_1)$ and $\bar{R}_{peak}(x_2)$;

3): If $\bar{R}_{peak}(x_1) = \bar{R}_{peak}(x_2)$, it means that we have get the accurate velocity. Considering the effect of thermal noise, we compare $|\bar{R}_{peak}(x_1)/\bar{R}_{peak}(x_2) - 1|$ with a small number ε, (in this pager, $\varepsilon = 0.0001$). If $|\bar{R}_{peak}(x_1)/\bar{R}_{peak}(x_2) - 1| < \varepsilon$, we go to 5), otherwise to 4);

4): If $\bar{R}_{peak}(x_1) < \bar{R}_{peak}(x_2)$, let $v_a = v_a, v_b = x_2$; otherwise if $\bar{R}_{peak}(x_1) > \bar{R}_{peak}(x_2)$, let $v_a = x_1, v_b = v_b$. Then we go back to 2);

5): $x = (x_1 + x_2)/2$ is the accurate estimation of velocity.

4.2. Coherent Bandwidth Synthesis

After motion compensation with the final velocity estimation, we can get the spectrum of each subpulse. The spectrum of all subpulses are coherently synthesized to form a much wider signal spectrum. The formulation of synthesized spectrum is

$$S_{syn}(f) \approx \sum_{n=1}^{N}\sum_{k=1}^{K} \tilde{A}_k \left| S(t_n, f - c_n \Delta f) \right|^2 \cdot \exp\left\{ \frac{-j4\pi[f - c_n \Delta f]\Delta R_k}{c} \right\} \quad (31)$$

Then the HRR imaging is obtained by performing IFFT operation on $S_{syn}(f)$ [15]

$$s(t) = \mathrm{IFFT}\{S_{syn}(f)\} \quad (32)$$

5. Numerical Simulation and Discussion

The transmitted radar waveform is shown in Figure 4, it's easy to see the baseband SCFM signals are random waveforms.

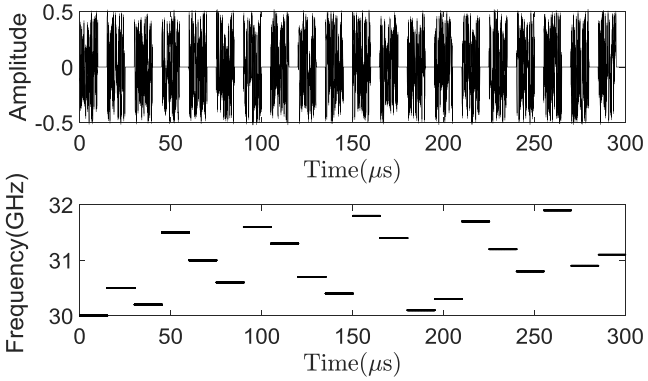

Figure 4. Transmitted Radar Waveforms, (A) The Inphase Components of SCFM Signals, (B) The Carrier Frequencies

Table 1 lists the simulation parameters. The subpulse bandwidth $B = 105$ MHz and the bandwidth of synthesized signal $B_{syn} = 2005$ MHz, which corresponding range resolution are about 1.5 m and 0.075 m, respectively.

Table 1. Simulation Parameters

parameters	values
T_p	10 μs
T_r	15 μs
B	105 MHz
f_0	30 GHz
Δf	100 MHz
N	20
B_{syn}	2005 MHz
Targets position	[3688, 3688.5, 3698, 3699] m
Radar cross section	[1.0, 1.0, 1.0, 1.0]
Velocity	6300 m/s
SNR	10 dB

In coarse search, we should first determine the search step (SS) and threshold of peak-average ration (PAR), in this paper, SS=121 m/s and PAR=20 dB, respectively. Figure 5 gives the search processes and results. It is clear that when $\left|v_{ref}-v\right|>dv$, the PARs are much smaller than 20 dB. However, when $\left|v_{ref}-v\right|<dv$, the PARs are very close to 20 dB, or even larger than 20 dB. In the end, the coarse velocity estimation is 6050 m/s, and the corresponding PAR is 23.15 dB.

Table 2 lists the results of accurate velocity search. The GSS algorithm can ensure the estimation converge to the true value with the search goes on, and finally an accurate velocity estimation (6295.19+6305.49)/2=6300.34 m/s is obtained with a small relative error of just 0.0054%.

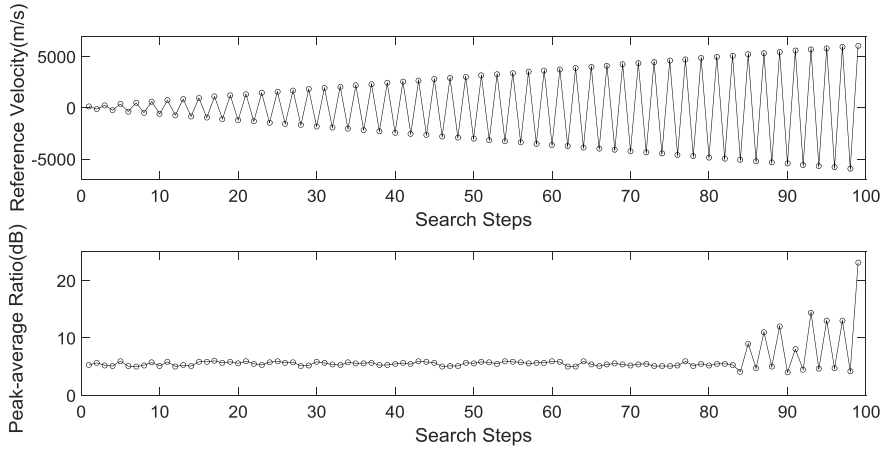

Figure 5. The Coarse Search

The phase induced by Doppler shift can be accurately compensated with the precise velocity estimation. Then, we can synthesize coherently wide band signal, whose bandwidth is about 2 GHz, as shown in Figure 6 and Figure 7 shows the range imaging result.

Table 2. GSS and Results

Search No.	1	2	3	4	5
v_a (m/s)	6050.00	6234.89	624.89	6234.89	6234.89
v_a (m/s)	6534.00	6534.00	6419.74	6349.13	6305.49
$\frac{\bar{R}_{peak}(x_1)}{\bar{R}_{mean}(x_2)}$	0.10507	0.95034	0.96352	0.96237	1.10257
Search No.	6	7	8	9	
v_a (m/s)	6261.86	6278.52	6288.82	6295.19	
v_a (m/s)	6305.49	6305.49	6305.49	6305.49	
$\frac{\bar{R}_{peak}(x_1)}{\bar{R}_{mean}(x_2)}$	1.10743	1.10463	1.09361	1.00003	

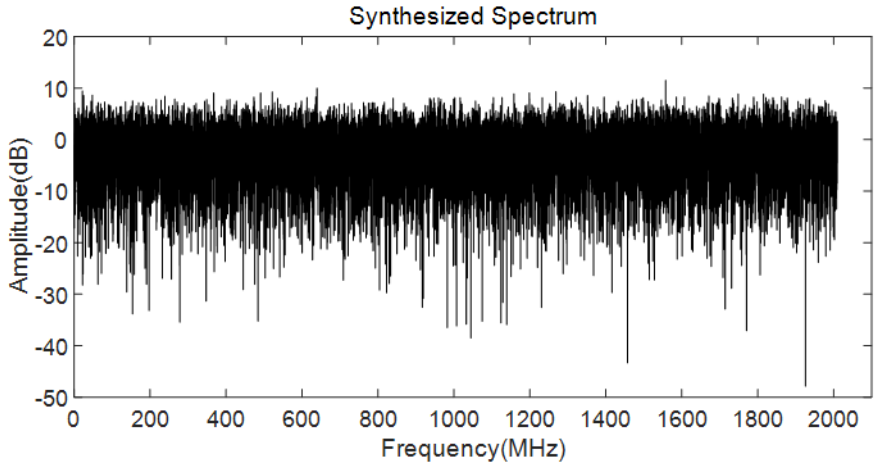

Figure 6. Synthesized Spectrum

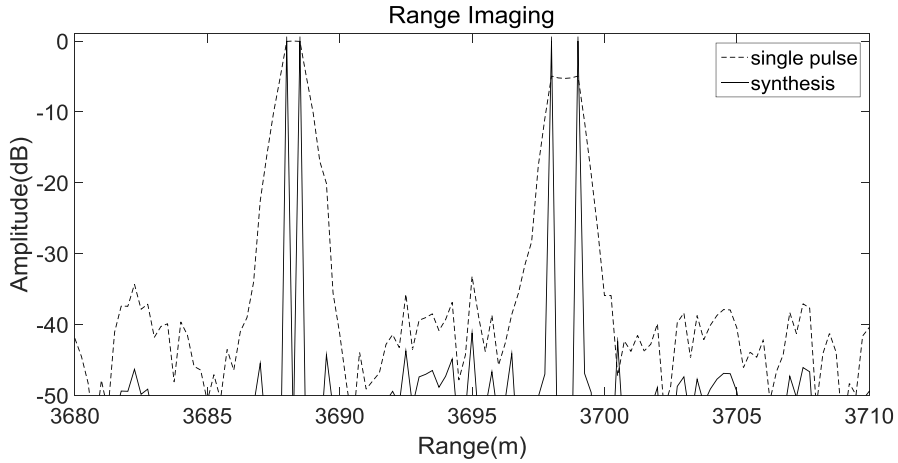

Figure 7. Range Imaging of Moving Targets

According to table 1, the distance between the first and the second and that between the third and the fourth are all less than 1.5m, the range resolution of a single subpulse. Consequently, we cannot distinguish the first and the second targets using just a single subpulse, the same to the third and fourth. However, as for the synthesized wideband signal, whose bandwidth $B_{syn} = 2005$ MHz, which corresponding range resolution is about 0.075m, so four targets can be clearly distinguished.

6. Conclusion

A novel radar waveform model based on stochastic chaotic signals is proposed, which can be used to estimate the velocity and HRR imaging of moving targets. SCS sequence is used to control the stepping of carrier frequencies and SCFM signal to be baseband noise signal.

Based on the proposed radar waveform, we present a search algorithm to velocity estimation, which consists of two steps: a coarse and a precise search. The two-stage search algorithm can ensure the estimation result converge to the true velocity. After phases compensation for all the subpulses with the accurate velocity estimation, the echoes are coherently synthesized and HRR imaging can be achieved. Simulation results demonstrate the effectiveness of the proposed model and algorithm.

Acknowledgment

This work was supported by the Educational Commission of Fujian Province, China (No.JA13235). Natural Science Foundation of Fujian Province, China (No.2015J01670).

References

[1] B. Horton, “Noise-modulated distance measuring systems”, Proceedings of the IRE, vol. 47, **(1959)**, pp. 821-828.
[2] S. E. Craig, W. Fishbein and O. Rittenbach, “Continuous-wave radar with high range resolution and unambiguous velocity determination”, Military Electronics, IRE Transactions on, vol. 1051, **(1962)**, pp.153-161.
[3] L. Guosui, G. Hong and S. Weimin, “Development of random signal radars”, Aerospace and Electronic Systems, IEEE Transactions on, vol. 35, **(1999)**, pp. 770-777.
[4] D. S. Garmatyuk and R. M. Narayanan, “ECCM capabilities of an ultrawideband bandlimited random noise imaging radar”, Aerospace and Electronic Systems, IEEE Transactions on, vol. 38, **(2002)**, pp.1243-1255.
[5] J. Yang, L. Nie, Z. Qiu, X. Li and Z. Zhuang, “Frequency modulated radar waveform based on sampled chaotic series”, Chinese Journal of Electronics, vol. 22, **(2013)**, pp. 426-432.
[6] Q. Yang, Y. Zhang and X. Gu, “A signal model based on combination chaotic map for noise radar”, Progress In Electromagnetics Research M, vol. 28, **(2013)**, pp. 57-71.
[7] C. S. Pappu and B. C. Flores, “Generation of high-range resolution radar signals using the Lorenz chaotic flow”, in SPIE Defense, Security, and Sensing, **(2010)**, pp. 76690T-76690T-12.
[8] M. S. Willsey, K. M. Cuomo and A. V. Oppenheim, “Quasi-orthogonal wideband radar waveforms based on chaotic systems”, Aerospace and Electronic Systems, IEEE Transactions on, vol. 47, **(2011)**, pp.1974-1984.
[9] B. Chen, “Improving autocorrelation and RFM autocorrelation performance of Skew tent sequence”, in Network Computing and Information Security (NCIS), 2011 International Conference on, **(2011)**, pp. 298-301.
[10] S. Xie, Z. He, J. Hu, L. Liu and J. Pan, “Performances of improved Tent chaos-based FM radar signal”, Journal of Systems Engineering and Electronics, vol. 23, **(2012)**, pp.1-5.
[11] R. J. Ma, H. S. Zhang and X. F. Mao, “Study on the Recognition of Electrogastric Signals Combining Multiple Decomposition Features”, Revista de la Facultad de Ingeniería, vol. 31, no. 6, **(2016)**, pp. 157-165.
[12] Q. Zhang, T. S. Yeo and G. Du, “ISAR imaging in strong ground clutter using a new stepped-frequency signal format”, Geoscience and Remote Sensing, IEEE Transactions on, vol. 41, **(2003)**, pp. 948-952.
[13] S. R. Axelsson, “Analysis of ultra wide band noise radar with randomized stepped frequency”, in Radar Symposium, 2006. IRS 2006. International, **(2006)**, pp. 1-4.
[14] Z. Liu, B. Deng and X. Wei, “Modified stepped-frequency train of LFM pulses”, in Information and Automation, 2008. ICIA 2008. International Conference on, **(2008)**, pp. 1137-1141.
[15] N. Levanon, "Stepped-frequency pulse-train radar signal”, IEE PROCEEDINGS Radar Sonar And Navigation, vol. 149, **(2002)**, pp. 297-309.
[16] J. Hu and T. H. Wang, “In situ impulse response method of oblique incidence sound absorption coefficient with microphone array”, Revista de la Facultad de Ingeniería, vol. 31, no. 5, **(2016)**, pp. 69-80
[17] Y. Tao1a, C. Long, F. You-Qian, L. Chang-Dong and Z. Feng, “A coherent jamming approach of frequency-stepped chirp ISAR”, Modern Radar, vol. 7, **(2010)**, pp.13-19.
[18] X. Gu, Y. Zhang, and X. Zhang, “Stepped frequency random noise uwb radar signal”, in Synthetic Aperture Radar (APSAR), 2011 3rd International Asia-Pacific Conference on, **(2011)**, pp. 1-4.

[19] P. González-Blanco, E. De Diego, E. Millán, B. Errasti and I. Montiel, "Stepped-frequency waveform radar demonstrator and its jamming", in Waveform Diversity and Design Conference, 2009 International, **(2009)**, pp. 192-196.
[20] P. Stein and S. M. Ulam, "Non-linear transformation studies on electronic computers", Los Alamos Scientific Lab., N. Mex, **(1962)**.
[21] J. A. González and R. Pino, "A random number generator based on unpredictable chaotic functions", Computer Physics Communications, vol. 120, **(1999)**, pp.109-114.
[22] J. A. González and R. Pino, "Chaotic and stochastic functions", Physica A: Statistical Mechanics and its Applications, vol. 276, **(2000)**, pp.425-440.
[23] Q. Xu, S. Dai, W. Pei, L. Yang and Z. He, "A Chaotic map based on scaling transformation of nonlinear function", Neural Information Processing-Letters and Reviews, vol. 3, **(2004)**, pp. 21-29.
[24] M. A. Richards, Fundamentals of radar signal processing: Tata McGraw-Hill Education, **(2005)**.
[25] N. Levanon, "Radar principles", New York, Wiley-Interscience, **(1988)**.
[26] W. Du, W. Han and Y. F. Tan, "Improved Golden Section Application in Maximum Power Point Tracking of Photovoltaic Power Generation", in Advanced Materials Research, **(2014)**, pp. 52-56.

Author

Jun Tang, he was born in 1977. He received the B.S. degree from Lanzhou University of Technology in 2000, and received the M.S. degree from Xidian University in 2007. He is currently a Ph.D. candidate in Communication Engineering from the Xiamen University (XMU). His research interest is radar signal processing.

